

Phylogenomics of Parasitic and Nonparasitic Lice (Insecta: Psocodea): Combining Sequence Data and Exploring Compositional Bias Solutions in Next Generation Data Sets

ROBERT S. DE MOYA^{1,2,*}, KAZUNORI YOSHIZAWA³, KIMBERLY K.O. WALDEN¹, ANDREW D. SWEET⁴, CHRISTOPHER H. DIETRICH², AND KEVIN P. JOHNSON²

¹Department of Entomology, University of Illinois Urbana-Champaign, 505 S. Goodwin Ave., Urbana, IL 61801, USA;

²Illinois Natural History Survey, Prairie Research Institute, University of Illinois, Champaign, IL 61820, USA;

³Systematic Entomology, School of Agriculture, Hokkaido University, Sapporo 060-8589, Japan; and

⁴Department of Entomology, Purdue University, 901 W. State St., West Lafayette, IN 47907, USA

*Correspondence to be sent to: Department of Entomology, University of Illinois Urbana-Champaign, 505 S. Goodwin Ave., Urbana, IL 61801, USA; E-mail: rde-moya2@illinois.edu

Received 27 November 2019; reviews returned 18 September 2020; accepted 21 September 2020

Associate Editor: Thomas Buckley

Abstract.—The insect order Psocodea is a diverse lineage comprising both parasitic (Phthiraptera) and nonparasitic members (Psocoptera). The extreme age and ecological diversity of the group may be associated with major genomic changes, such as base compositional biases expected to affect phylogenetic inference. Divergent morphology between parasitic and nonparasitic members has also obscured the origins of parasitism within the order. We conducted a phylogenomic analysis on the order Psocodea utilizing both transcriptome and genome sequencing to obtain a data set of 2370 orthologous genes. All phylogenomic analyses, including both concatenated and coalescent methods suggest a single origin of parasitism within the order Psocodea, resolving conflicting results from previous studies. This phylogeny allows us to propose a stable ordinal level classification scheme that retains significant taxonomic names present in historical scientific literature and reflects the evolution of the group as a whole. A dating analysis, with internal nodes calibrated by fossil evidence, suggests an origin of parasitism that predates the K-Pg boundary. Nucleotide compositional biases are detected in third and first codon positions and result in the anomalous placement of the Amphientometae as sister to Psocomorpha when all nucleotide sites are analyzed. Likelihood-mapping and quartet sampling methods demonstrate that base compositional biases can also have an effect on quartet-based methods. [Illumina; Phthiraptera; Psocoptera; quartet sampling; recoding methods.]

The era of phylogenomic analysis has provided access to new data types originating from different genomic regions [e.g., ultraconserved elements (UCE) and single-copy protein-coding orthologs] (Jarvis et al. 2014; Prum et al. 2015) or from post-transcriptional processes (i.e., transcriptomes) (Misof et al. 2014; Johnson et al. 2018a). Availability of certain data types may be contingent on the quality or age of a specimen. For example, RNA degrades quickly, and transcriptome-based analyses are not typically feasible for old or fixed specimens (Houseley and Tollervey 2009; Bossert et al. 2019). Transcriptomes are obtainable for fresh specimens preserved in an appropriate buffer (e.g., RNA-later™) that inhibits the activity of RNases which degrade RNA (Houseley and Tollervey 2009). Transcriptomes correspond to coding gene sequences and are free of noncoding introns, and thus align well. Alternatively, most next generation methods that produce whole genome sequences include a fragmentation step prior to library construction (Alkan et al. 2011) that may mimic degradation processes that occur in specimens that are dry or old (Bossert et al. 2019). DNA-based genome sequencing is not limited by the amount of RNA present in a cell and can produce many reads across the genome (Johnson 2019). However, raw genomic DNA sequence data contain intron and noncoding data (Jarvis et al. 2014), but these can be excised prior or masked following alignment with transcriptome data. High-volume sequencing technologies have often been described and implemented in phylogenomic studies; however,

approaches to combine sequences derived from different next generation sequencing technologies have been less developed. A recent phylogenomic analysis of Apidae (bees) successfully combined transcriptome, genome, and UCE data to produce a robust topology (Bossert et al. 2019). However, this is one of few studies to combine transcriptome and partial genome data in a single phylogenomic analysis.

Phylogenomic analyses have helped resolve many contentious relationships but have also accentuated the need to test for compositional (and other) biases in molecular data sets that may be amplified by the inclusion of millions of base pairs of nucleotides and can lead to strong support for misleading hypotheses (Romiguier et al. 2016; Bossert et al. 2017, 2019; Simion et al. 2017; Laumer et al. 2018; Simon et al. 2018; Vasilikopoulos et al. 2019). Before the widespread use of phylogenomic analysis, Sanger sequencing-based phylogenetics sought to optimize the topology by testing hierarchical models of evolution (Posada and Crandall 1998). Weaknesses of these models can be exposed (Duchêne et al. 2017), due to large-scale compositional biases that exist in codon positions found across thousands of loci, which violate model assumptions of stationarity (Simion et al. 2017; Laumer et al. 2018). These biases can create phylogenetic artifacts that appear well supported given traditional clade support values (i.e., bootstrap support) but is actually misleading because the large amount of data simply converges upon a stable topology due to underlying weaknesses in model assumptions.

Base compositional biases (%GC) have long been known to influence the results of phylogenetic analyses (Galtier and Gouy 1995; Jermin et al. 2004; Bossert et al. 2017) and several methods for reducing the influence of such biases on phylogenetic inference have been proposed (Jermin et al. 2004; Sheffield et al. 2009; Regier et al. 2010; Ishikawa et al. 2012; Zwick et al. 2012; Simmons 2017). However, most methods that incorporate time-heterogeneous approaches (Philippe et al. 2011; Roure and Philippe 2011) are extremely computationally intensive and would be difficult to apply to large phylogenomic data sets, although they have been applied in mitochondrial phylogenomics with success (Sheffield et al. 2009). Alternative methods include recoding techniques (Simmons 2017) which use IUPAC ambiguity codes to mask variable codon positions that code for a silent mutation, such as RY recoding (Ishikawa et al. 2012) and degeneracy methods (Regier et al. 2010; Zwick et al. 2012). Another solution is to discard possible saturated data, for example removal of the third codon positions from an alignment (Breinholt and Kawahara 2013) or even the first and third codon positions (Misof et al. 2014). These two methods are effective for concatenated data sets; however, coalescent analyses may also be influenced by compositional biases in individual genes (Romiguier et al. 2016; Bossert et al. 2017, 2019). A further solution is to analyze amino acid sequences, although it is possible that underlying base compositional biases can result in amino acid biases as well (Foster et al. 1997). In addition, molecular models for the evolution of amino acids are much more computationally intensive and may not be feasible for analysis of large genomic data sets, because a 21 amino acid model (two coding strategies for serine) (Zwick et al. 2012) is much more complex relative to nucleotide models based on four bases (Posada and Crandall 1998). Here, we explore some of these issues using a combined genome and transcriptome data set for a group of insects (Psocodea) known to have strong variation in base compositional biases across taxa (Johnson et al. 2003; Yoshizawa and Johnson 2013).

The insect order Psocodea encompasses the two historically recognized groups Psocoptera (free-living bark lice) and Phthiraptera (parasitic lice) that were once considered separate orders. Members of Psocodea have an extensive fossil record that extends into the Lower Cretaceous (Mockford et al. 2013) and molecular divergence time estimates place their origin in the Paleozoic (~404 Ma) (Misof et al. 2014; Johnson et al. 2018a; Yoshizawa et al. 2019). The order also encompasses species with a range of feeding preferences, from detritus, plant material (i.e., pollen, decaying leaves), and microflora (i.e., cyanobacteria films, fungal, and lichen) in nonparasitic members (Broadhead and Wapshere 1966; New 1970, 1987; Broadhead and Richards 1982); to obligate ectoparasitism on birds and mammals (i.e., skin debris, feathers, blood/skin secretions) (Price et al. 2003; Clayton et al. 2015). The ecological diversity and age of the group have likely contributed to large-scale compositional biases that have previously been detected

between parasitic and nonparasitic members (Johnson et al. 2003; Yoshizawa and Johnson 2013; Johnson et al. 2018a). These known compositional biases provide an opportunity to examine the effects such biases may have on phylogenomic analyses. Other groups of organisms are also known to show such biases (Cox et al. 2014; Romiguier et al. 2016; Bossert et al. 2017; Skinner et al. 2020), thus understanding the potential effects and methods to account for such biases will have relevance to many phylogenomic studies.

The order Psocodea also represents an ideal taxon for examining the effect of combining whole genome and transcriptome derived sequence data. Parasitic lice are known to have reduced genome sizes (Pittendrigh et al. 2006; Johnston et al. 2007; Kirkness et al. 2010) and are minute insects which typically produce small amounts of RNA. *Pediculus humanus* has one of the smallest insect genomes recorded, at 108 Mbp (Kirkness et al. 2010), and coverage estimates from Illumina genome sequencing indicate small genome sizes may be a general feature of Psocodea (100–400 Mbp, unpublished). While it has been possible in the past to sequence transcriptome-based data for parasitic Phthiraptera based on pooling many individuals (Johnson et al. 2018b), data are more readily obtained by whole genome sequencing (Allen et al. 2017; Boyd et al. 2017; Sweet et al. 2018). The reduced genome size of parasitic lice makes it possible to produce high quality assemblies from multiplexed samples on a single sequencing lane with whole genome-based sequencing methods (Allen et al. 2017; Boyd et al. 2017; Sweet et al. 2018; Johnson 2019). In contrast, nonparasitic Psocodea (bark lice) are typically larger in body volume and produce higher copy transcript sequences (Johnson et al. 2018a). Less total sequence data are needed for transcriptome sequencing thus are more economical than whole genome sequencing. (Johnson 2019). Therefore, there is a cost advantage to combining transcriptome and whole genome data in phylogenomic analyses that combine parasitic and nonparasitic Psocodea. Our study is the first to test the utility of combining these different data types in a study of Psocodea phylogeny, and this general approach should be applicable to many groups of organisms.

Although the monophyly of the lineage comprising both Phthiraptera and Psocoptera is well established based on morphological criteria (Lyal 1985; Yoshizawa and Lienhard 2010), inconsistent taxonomic treatment of the two groups continues (Emeljanov et al. 2001; Scholtz 2016; Durden 2019; Wang et al. 2019). Psocoptera traditionally consists of three recognized suborders (Trogiomorpha, Psocomorpha, and Troctomorpha) (Lienhard and Smithers 2002) and Phthiraptera has four previously recognized suborders (Amblycera, Ischnocera, Rhynchophthirina, and Anoplura) (Price et al. 2003). Based on molecular and morphological evidence, Phthiraptera is derived from within the Troctomorpha (Lyal 1985; Johnson et al. 2004; Yoshizawa and Johnson 2010; Johnson et al. 2018a), but inconsistent use of the subordinal ranks that divide the traditional orders Psocoptera and Phthiraptera can be found in modern

literature (Emeljanov et al. 2001; Scholtz 2016). Adding to the confusion, the origin of parasitism remains in question (Yoshizawa and Johnson 2010) because phylogenetic analyses of a ribosomal gene suggested that Phthiraptera could be polyphyletic (Johnson et al. 2004).

To explore the phylogenetic relationships within Psocodea, we assembled a large phylogenomic data set (2370 orthologous genes) derived from whole genome and transcriptome sequencing using a customized pipeline. Using this data set, comprising more than two million base pairs of nucleotide data, we examined the effects of large base compositional biases on phylogenetic inference. We used the results from our assessment of the influence of base composition on tree topology to conduct a dating analysis accounting for these biases to explore the origins of parasitism in this group.

MATERIALS AND METHODS

Taxonomic Sampling

Sampling was aimed at resolving deep level relationships between historically recognized orders or suborders that comprise the insect order Psocodea. One focus of the sampling was resolving whether or not the parasitic lice (Phthiraptera) form a monophyletic assemblage (Johnson et al. 2004; Yoshizawa and Johnson 2010). Sampling included a broad array of parasitic species and the closest nonparasitic members known as the Nanopsocetae (Mockford 1993). In total 112 individuals were sampled, encompassing all currently recognized suborders and infraorders (Table 1). Prior studies established that Trogiomorpha is monophyletic and is the sister taxon of the remainder of Psocodea (Johnson et al. 2004; Yoshizawa et al. 2006), so we used this suborder as the root. This was done because the sister taxon of Psocodea is currently unclear (Misof et al. 2014; Johnson et al. 2018a), thus we avoided outgroups that are highly divergent from the ingroup to circumvent alignment difficulties and potential long-branch attraction artifacts.

Next Generation Sequencing and Orthology Inference

Given the inherent difficulties of obtaining large quantities of freshly preserved tiny insects, such as lice, we developed a pipeline to use whole genome sequencing to obtain orthologs belonging to a set included in a previous data set derived from transcriptome data (Johnson et al. 2018a). In some cases, both genome and transcriptome sequences were available for the same species. This allowed us to verify that these two data types placed respective species in the same phylogenetic position.

Whole genome data were obtained following genomic DNA extraction procedures and using Illumina sequencing technologies. Specimens were stored in 95% ethanol at -80°C . From these, genomic DNA was extracted using a Qiagen DNAeasy extraction kit. The protocol was slightly modified with an extended 48-h incubation step and use of 52 μL of elution buffer. DNA was quantified using a Qubit 3.0 fluorometer. The extractions

were then sonicated with a Covaris M220 to an average size of 300–400 nt. A Kapa Library Preparation Kit (Kapa Biosystems) was used to produce paired-end libraries. The libraries were then pooled into equimolar concentrations, quantified by qPCR. Each sample was sequenced for 151–161 cycles on a HiSeq2500 (Illumina) with a TruSeq or HiSeq SBS sequencing rapid kit to produce 150 or 160 nt reads. Fastq files were produced with Casava 1.8.2 or bcl2fastq v2.17.1.14. Adaptors and low-quality bases were removed using the FASTX Toolkit 0.0.14 (Gordon and Hannon 2010). All sequencing took place at W.M. Keck Center at the University of Illinois, Urbana-Champaign. A gene set of 2395 protein-coding orthologs previously used for phylogenomic analyses of hemipteroid insects was identified in the annotated genome of the human body louse, *P. humanus* (Johnson et al. 2018a). This ortholog set was used as a reference in aTRAM 1.0 (Allen et al. 2015) for local assembly of individual orthologs. This software uses tblastn searches to identify reads matching the gene of interest and assembles them locally. Parameters for aTRAM loci assembly were set to three iterations, fraction one, and the ABySS de novo assembler (Simpson et al. 2009). Exon sequences assembled by aTRAM were then annotated and stitched together if needed using an Exonerate-based (Slater and Birney 2005) pipeline (Allen et al. 2017). Transcriptome assemblies and inferred ortholog transcripts were previously published (Table 1, Johnson et al. 2018a).

Phylogenomic Analyses

Nucleotide sequences inferred as being orthologous from whole genome sequence data were translated with Geneious 11.1.15 (Kearse et al. 2012). Translated whole genome and transcriptome sequences were aligned with PASTA 1.8.0 by amino acid with memory usage increased (2048 MB) and otherwise default parameters (Mirarab et al. 2014a). Nucleotide sequences were retrieved using a custom python script to produce a final nucleotide alignment based upon the amino acid alignments (Allen et al. 2017). Exonerate inserts ambiguous N's between combined exon data, therefore excess N's were recoded to gaps before subsequent masking. Multiple sequence gene alignments (MSAs) were masked on a nucleotide level with trimAl (Capella-Gutiérrez et al. 2009) using a 40% gap threshold. MSAs that included less than 50% of individuals were eliminated from subsequent analyses. Final concatenated supermatrices of 2370 gene sequences were produced with SequenceMatrix 1.8 (Vaidya et al. 2011).

Several phylogenetic analyses were performed using the final nucleotide supermatrix. First, all nucleotide sites were analyzed in both partitioned and unpartitioned maximum likelihood (ML) frameworks. Second, nucleotide sites were recoded using degeneracy coding (Regier et al. 2010; Zwick et al. 2012) for phylogenetic analyses. Finally, nucleotide supermatrices of 1) first and second codon positions and 2) second codon positions only were produced from Geneious (Kearse et al. 2012). Partitioned analyses were performed on the all

TABLE 1. A summary of all species of Psocodea sampled and data analyzed.

Psocodea taxonomic sampling scheme						
Suborder or order	Family	Taxon	Data	Total BP	No. of genes	SRA accession
Anoplura	Haematopinidae	<i>Haematopinus eurysternus</i>	WGS	2,549,976	2357	SRR5308123
Anoplura	Echinophthiriidae	<i>Proechinophthirus fluctus</i>	WGS	2,253,525	2335	SRR5308138
Anoplura	Echinophthiriidae	<i>Antarctophthirus microchir</i>	WGS	2,440,791	2349	SRR5088465
Anoplura	Echinophthiriidae	<i>Echinophthirus horridus</i>	RNA seq	785,123	1599	SRR2051484
Anoplura	Linognathidae	<i>Linognathus spicatus</i>	WGS	2,567,331	2332	SRR5308129
Anoplura	Polyplacidae	<i>Neohaematopinus pacificus</i>	WGS	2,787,132	2364	SRR5088469
Anoplura	Hoplopleuridae	<i>Hoplopleura arboricola</i>	WGS	2,336,922	2359	SRR5088468
Anoplura	Pedicinidae	<i>Pedicinus badius</i>	WGS	2,344,773	2356	SRR5308136
Anoplura	Pthiridae	<i>Pthirus gorillae</i>	WGS	2,789,559	2368	SRR5088474
Anoplura	Pthiridae	<i>Pthirus pubis</i>	WGS	2,754,231	2365	SRR5088475
Anoplura	Pediculidae	<i>Pediculus schaeffi</i>	WGS	2,562,033	2364	SRR1182279
Anoplura	Pediculidae	<i>Pediculus humanus</i>	WGS	2,277,984	2354	SRR5088472
Anoplura	Pediculidae	<i>Pediculus humanus</i>	Reference	2,945,068	2370	PRJNA19807
Rhynchophthirina	Haematomyzidae	<i>Haematomyzus elephantis</i>	WGS	2,439,042	2358	SRR5308122
Rhynchophthirina	Haematomyzidae	<i>Haematomyzus elephantis</i>	RNA seq	1,194,114	1867	SRR2051491
Ischnocera	Trichodectidae	<i>Stachiella larseni</i>	WGS	2,524,617	2353	SRR5308143
Ischnocera	Trichodectidae	<i>Geomydoecus aurei</i>	WGS	2,507,592	2355	SRR5308121
Ischnocera	Trichodectidae	<i>Geomydoecus ewingi</i>	RNA seq	2,596,821	2310	SRR1821919
Ischnocera	Philopteridae	<i>Trichophilopterus babakotophilus</i>	WGS	2,497,134	2359	SRR5308144
Ischnocera	Philopteridae	<i>Bothriometopus macrocnemis</i>	WGS	1,835,208	2259	SRR5088466
Ischnocera	Philopteridae	<i>Craspedonirmus immer</i>	WGS	2,193,294	2348	SRR5308116
Ischnocera	Philopteridae	<i>Columbicola columbae</i>	WGS	2,225,532	2356	SRR5308115
Ischnocera	Philopteridae	<i>Columbicola columbae</i>	RNA seq	1,968,492	2218	SRR1821984
Ischnocera	Philopteridae	<i>Docophoroides brevis</i>	WGS	2,313,018	2355	SRR5308117
Ischnocera	Philopteridae	<i>Halipeurus diversus</i>	WGS	2,281,860	2354	SRR5308124
Ischnocera	Philopteridae	<i>Fulicoffula longipila</i>	WGS	2,129,253	2345	SRR5308119
Ischnocera	Philopteridae	<i>Anatoecus icterodes</i>	WGS	2,208,450	2338	SRR5308111
Ischnocera	Philopteridae	<i>Falcolipeurus marginalis</i>	WGS	2,280,087	2350	SRR5308118
Ischnocera	Philopteridae	<i>Ibidoecus bisignatus</i>	WGS	2,341,512	2353	SRR5308126
Ischnocera	Philopteridae	<i>Pectinopygus varius</i>	WGS	2,034,798	2315	SRR5308135
Ischnocera	Philopteridae	<i>Chelopistes texanus</i>	WGS	2,589,447	2363	SRR5308114
Ischnocera	Philopteridae	<i>Oxylipeurus chiniri</i>	WGS	2,668,434	2368	SRR5308134
Ischnocera	Philopteridae	<i>Degeeriella rufa</i>	WGS	2,485,305	2353	SRR5088467
Ischnocera	Philopteridae	<i>Brueelia antiqua</i>	WGS	2,700,864	2357	SRR5308112
Ischnocera	Philopteridae	<i>Penenirmus auritus</i>	WGS	2,497,635	2361	SRR5308137
Ischnocera	Philopteridae	<i>Alcedoecus</i> sp.	WGS	2,417,226	2359	SRR5308110
Ischnocera	Philopteridae	<i>Quadriceps punctatus</i>	WGS	2,566,107	2362	SRR5308139
Ischnocera	Philopteridae	<i>Saemundssonina lari</i>	WGS	2,501,502	2353	SRR5308141
Ischnocera	Philopteridae	<i>Goniodes ortygis</i>	WGS	2,498,694	2356	SRR5308120
Ischnocera	Philopteridae	<i>Campanulotes compar</i>	WGS	2,336,796	2355	SRR5308113
Ischnocera	Philopteridae	<i>Campanulotes compar</i>	RNA seq	2,134,521	2251	SRR1821983
Ischnocera	Philopteridae	<i>Strongylocotes lipogonus</i>	WGS	2,739,207	2363	SRR5308142
Ischnocera	Philopteridae	<i>Megaginus tataupensis</i>	WGS	2,582,559	2364	SRR5308131
Ischnocera	Philopteridae	<i>Pessoaiella absita</i>	WGS	2,403,510	2358	SRR5308145
Ischnocera	Philopteridae	<i>Osculotes curta</i>	WGS	2,480,868	2363	SRR5308133
Ischnocera	Philopteridae	<i>Craspedorrhynchus</i> sp.	RNA seq	2,560,936	2301	SRR1821912
Amblycera	Ricinidae	<i>Ricinus</i> sp.	WGS	2,187,996	2310	SRR5308140
Amblycera	Menoponidae	<i>Osborniella crotophagae</i>	WGS	2,399,703	2342	SRR5088470
Amblycera	Menoponidae	<i>Myrsidea</i> sp.	WGS	1,997,502	2284	SRR5308132
Amblycera	Menoponidae	<i>Menopon gallinae</i>	RNA seq	2,405,619	2263	SRR921619
Amblycera	Boopiidae	<i>Heterodoxus spiniger</i>	WGS	2,451,921	2340	SRR5308125
Amblycera	Trimenoponidae	<i>Cummingsia maculata</i>	WGS	2,314,959	2335	SRR5308146

(Continued)

TABLE 1. Continued

Suborder or order	Family	Taxon	Data	Total BP	No. of genes	SRA accession
Amblycera	Gyropidae	<i>Macrogyropus costalimai</i>	WGS	2,432,211	2347	SRR5308130
Amblycera	Laemobothriidae	<i>Laemobothrion tinnunculi</i>	WGS	2,425,458	2344	SRR5308127
Troctomorpha	Liposcelididae	<i>Liposcelis brunnea</i>	WGS	2,112,042	2329	SRR5308128
Troctomorpha	Liposcelididae	<i>Liposcelis pearmani</i>	WGS	2,199,234	2346	SRR5308268
Troctomorpha	Liposcelididae	<i>Liposcelis bostrychophila</i>	RNA seq	2,125,494	2201	SRR921613
Troctomorpha	Liposcelididae	<i>Embidopsocus</i> sp. 2	WGS	2,330,187	2353	SRR5308269
Troctomorpha	Liposcelididae	<i>Embidopsocus</i> sp. 2	RNA seq	2,557,295	2318	SRR5134727
Troctomorpha	Liposcelididae	<i>Embidopsocus</i> sp.	RNA seq	963,150	1709	SRR2051486
Troctomorpha	Pachytroctidae	<i>Pachytroctes maculosus</i>	WGS	2,317,935	2313	SRR5308279
Troctomorpha	Pachytroctidae	<i>Tapinella</i> sp.	WGS	2,370,138	2336	SRR5308286
Troctomorpha	Pachytroctidae	<i>Peritroctes</i> sp.	WGS	2,442,492	2340	SRR5308280
Troctomorpha	Sphaeropsocidae	<i>Badonnelia titei</i>	WGS	2,394,783	2343	SRR5308262
Troctomorpha	Sphaeropsocidae	<i>Badonnelia titei</i>	RNA seq	2,183,178	2186	SRR2051472
Troctomorpha	Amphientomidae	<i>Stimulopalpus japonicus</i>	WGS	2,270,973	2300	SRR5088476
Troctomorpha	Amphientomidae	<i>Stimulopalpus japonicus</i>	RNA seq	1,828,280	2061	SRR2051511
Troctomorpha	Musapsocidae	<i>Musapsocus</i> sp.	WGS	2,363,169	2348	SRR5308275
Troctomorpha	Compsocidae	<i>Compsocus elegans</i>	WGS	2,367,267	2322	SRR5308266
Troctomorpha	Electrentomidae	<i>Epitroctes</i> sp.	WGS	2,400,144	2330	SRR5308270
Psocomorpha	Elipsocidae	<i>Kilauella</i> sp.	WGS	2,329,824	2313	SRR5308272
Psocomorpha	Elipsocidae	<i>Nepiomorpha</i> sp.	WGS	2,570,349	2309	SRR5308276
Psocomorpha	Elipsocidae	<i>Propsocus pulchripennis</i>	WGS	2,325,882	2309	SRR5308281
Psocomorpha	Elipsocidae	<i>Elipsocus kuriliensis</i>	RNA seq	1,843,671	2158	SRR2051485
Psocomorpha	Pseudocaeciliidae	<i>Calopsocus reticulatus</i>	WGS	2,301,513	2288	SRR5308264
Psocomorpha	Pseudocaeciliidae	<i>Bryopsocus townsendi</i>	WGS	2,188,992	2268	SRR5308263
Psocomorpha	Pseudocaeciliidae	<i>Heterocaecilius solocipennis</i>	RNA seq	1,906,914	2126	SRR2051493
Psocomorpha	Trichopsocidae	<i>Trichopsocus clarus</i>	WGS	2,332,443	2298	SRR5308287
Psocomorpha	Cladiopsocidae	<i>Cladiopsocus ocotensis</i>	WGS	2,312,040	2290	SRR5308265
Psocomorpha	Ptiloneuridae	<i>Loneura mombachensis</i>	WGS	2,059,170	2240	SRR5308274
Psocomorpha	Archipsocidae	<i>Archipsocus nomas</i>	WGS	2,373,123	2304	SRR5308260
Psocomorpha	Epipsocidae	<i>Neurostigma</i> sp.	WGS	2,158,530	2267	SRR5308277
Psocomorpha	Epipsocidae	<i>Bertkauia</i> sp.	RNA seq	1,686,357	1939	SRR2051473
Psocomorpha	Asiopsocidae	<i>Asiopsocus sonorensis</i>	WGS	2,368,782	2298	SRR5308261
Psocomorpha	Caeciliusidae	<i>Xanthocaecilius sommermanae</i>	WGS	2,256,093	2284	SRR5308288
Psocomorpha	Caeciliusidae	<i>Valenzuela badiostigma</i>	RNA seq	1,980,198	2179	SRR2051514
Psocomorpha	Lachesillidae	<i>Anomopsocus amabilis</i>	WGS	2,308,974	2294	SRR5308259
Psocomorpha	Lachesillidae	<i>Lachesilla contraforcepeta</i>	RNA seq	2,164,547	2279	SRR1821927
Psocomorpha	Lachesillidae	<i>Lachesilla abiesicola</i>	RNA seq	1,658,454	2106	SRR2051497
Psocomorpha	Mesopsocidae	<i>Idatenopsocus orientalis</i>	WGS	2,362,071	2302	SRR5308271
Psocomorpha	Mesopsocidae	<i>Mesopsocus unipunctatus</i>	RNA seq	1,546,809	1987	SRR2051502
Psocomorpha	Dasydemellidae	<i>Matsumuraiella radiopicta</i>	RNA seq	2,026,917	2212	SRR2051500
Psocomorpha	Psilopsocidae	<i>Psilopsocus</i> sp.	WGS	2,111,205	2239	SRR5308283
Psocomorpha	Stenopsocidae	<i>Graphopsocus cruciatus</i>	RNA seq	1,820,073	2095	SRR2051490
Psocomorpha	Amphipsocidae	<i>Amphipsocus japonicus</i>	RNA seq	2,010,662	2177	SRR2051466
Psocomorpha	Peripsoctidae	<i>Peripsoctes phaeopterus</i>	RNA seq	1,665,303	2038	SRR2051507
Psocomorpha	Ectopsocidae	<i>Ectopsocus briggsi</i>	RNA seq	1,870,215	2125	SRR645929
Psocomorpha	Psocidae	<i>Longivalvus nubilus</i>	RNA seq	1,299,474	1716	SRR2051498
Psocomorpha	Psocidae	<i>Ptycta johnsoni</i>	RNA seq	1,602,536	2006	SRR1821962
Psocomorpha	Psocidae	<i>Neoblaste papillosus</i>	RNA seq	1,716,579	2052	SRR2051505
Psocomorpha	Hemipsocidae	<i>Hemipsocus chloroticus</i>	RNA seq	1,638,022	2025	SRR2051492
Psocomorpha	Philotarsidae	<i>Aaroniella</i> sp.	RNA seq	1,578,200	1891	SRR2051465
Trogiomorpha	Prionoglarididae	<i>Speleketor irwini</i>	WGS	1,898,916	2200	SRR5308285
Trogiomorpha	Prionoglarididae	<i>Prionoglaris stygia</i>	WGS	2,282,502	2290	SRR5308282
Trogiomorpha	Prionoglarididae	<i>Neotroglia</i> sp.	WGS	1,977,267	2244	SRR5308278
Trogiomorpha	Prionoglarididae	<i>Neotroglia aurora</i>	RNA seq	1,725,501	2005	SRR5134732
Trogiomorpha	Psyllipsocidae	<i>Dorypteryx domestica</i>	WGS	2,330,406	2308	SRR5308267

(Continued)

TABLE 1. Continued

Suborder or order	Family	Taxon	Data	Total BP	No. of genes	SRA accession
Trogiomorpha	Psyllipsocidae	<i>Psyllipsocus ramburii</i>	RNA seq	2,394,803	2277	SRR5134716
Trogiomorpha	Psoquillidae	<i>Rhyopsocus</i> sp.	WGS	2,012,127	2213	SRR5308284
Trogiomorpha	Trogiidae	<i>Lepinotus patruelis</i>	RNA seq	2,391,270	2286	SRR5134710
Trogiomorpha	Trogiidae	<i>Cerobasis guestfalica</i>	RNA seq	1,947,314	2186	SRR2051476
Trogiomorpha	Lepidopsocidae	<i>Echmepteryx hageni</i>	RNA seq	1,546,566	1859	SRR1821982

Transcriptome sequences are available from a previous study (Johnson et al. 2018a).

nucleotide site and degeneracy recoded supermatrices. The optimal partitioning scheme was determined with PartitionFinder 2.1.1 (Lanfear et al. 2017) and the implemented version of RAxML 8.2.11 (Stamatakis 2014) with the following parameters: branch lengths linked, GTR + G model, Bayesian Information Criterion (BIC) model selection, rcluster search and max set to 100.

A series of ML phylogenetic analyses were performed on the resulting supermatrices using ExaML 3.0.21 (updated: 6/4/2018) (Kozlov et al. 2015) and RAxML 8.2.11 (Stamatakis 2014). To save computation time, the ML hill-climbing algorithm was performed in ExaML with a gamma model and 100 rapid bootstrap replicates were completed with RAxML using the GTR + G model with four GAMMA categories. For each bootstrap search, we tested for bootstrap convergence using RAxML (Pattengale et al. 2009). In all cases, convergence was reached by 50 replicates, so the 100 bootstrap replicates are sufficient to provide a reliable estimator of bootstrap proportions. To ensure that the most likely topology was obtained, eight separate tree searches were performed with ExaML, each with different starting input trees derived from RAxML (four parsimony based and four random start topologies). Bootstrap support (BS) for the most likely topology obtained was then mapped using SumTrees 4.1.0 (Sukumaran and Holder 2015). These methods were used to analyze all supermatrices produced (all nucleotide sites, degeneracy recoding, second codon positions only, and third codon positions removed).

To account for possible incongruence among genes due to incomplete lineage sorting or other biases masked by concatenation, we also performed coalescent gene/species-tree analyses using Astral 5.5.9 (Mirarab et al. 2014b; Mirarab and Warnow 2015). To infer individual gene trees as basis, each of the 2370 MSAs were analyzed with RAxML using GTR + G and 100 rapid bootstrap replicates. Estimation of individual gene trees was performed using both 1) all sites and 2) the degeneracy recoded data for each gene. Resulting bipartition files produced from RAxML were used as in input for Astral analyses using default parameters with branch support calculated based on local posterior probability (LPP) (Sayyari and Mirarab 2016).

To evaluate support for conflicting topologies surrounding the phylogenetic position of Amphientometae (see Results section) due to potential biases in the concatenated data set, quartet sampling (Pease et al. 2018)

and four cluster likelihood-mapping (quartet mapping, Strimmer and Haeseler 1997) methods were employed. Four cluster likelihood-mapping was performed in IQ-TREE 1.6.5 (Nguyen et al. 2015) testing all possible quartets, tree search skipped, GTR + G model, and the following quartets defined: Trogiomorpha, Psocomorpha, Amphientometae, and Nanopsocetae. Likelihood-mapping in IQ-TREE was performed on the nucleotide supermatrix with 1) all sites, 2) degeneracy recoding, 3) first and second positions only, and 4) second codon positions only. Four cluster likelihood-mapping is not computationally feasible across all branches in large data sets. However, Pease et al. (2018) developed a quartet sampling method which performs four cluster likelihood-mapping across each node of the tree but using a random subsample of all possible quartet combinations for that node. We used quartet sampling (Pease et al. 2018) to evaluate support for conflicting topologies across all phylogenetic branches. Quartet sampling was performed using a log likelihood cutoff value of 2 and 200 replicates per branch on the supermatrices for 1) all sites, 2) degeneracy recoding, 3) first and second positions only, and 4) second codon positions only. For ease of comparison, we provide a summary of all phylogenetic analyses performed (Table 2).

Guanine and cytosine content (GC%) were calculated per gene and codon position from the masked MSAs with a custom python script (Allen et al. 2015, 2017). Following GC% calculation, biases were visualized with box and whisker plots produced from RStudio 1.1.453 (RS Team 2015). Distribution of the GC% obtained for each individual gene were arranged in ascending order per individual sampled based on the median GC% score obtained. This process was repeated for first, second, and third codon positions.

Phylogenetic dating analyses using relaxed clock methods were performed with MCMCTree in the PAML package under a correlated rates model (Yang 2007) on a topology resulting from the ML searches of the partitioned degeneracy-coded data set. A total of nine internal calibration points with soft bounds were based on fossil evidence or previous dating analyses (Wappler et al. 2004; Mockford et al. 2013; Johnson et al. 2018a,b). The internal minimum age calibrations based on fossil evidence include the following: split of Atropetae (120 Ma), Psocomorpha (84 Ma), Caeciliusidae (33.9 Ma), Psocidae (33.9 Ma), Amphientometae (145 Ma),

TABLE 2. A summary of the phylogenetic analyses completed, and respective data type analyzed.

Summary of analyses completed				
Data type	Maximum likelihood	Astral	Quartet sampling	Likelihood-mapping
All sites	Partitioned and concatenated	Yes	Yes	Yes
Third positions removed	Concatenated only	No	Yes	Yes
Second positions only	Concatenated only	No	Yes	Yes
Degeneracy recoded	Partitioned and concatenated	Yes	Yes	Yes

Liposcelididae + Phthiraptera (99 Ma), Menoponidae (44 Ma), *Pedicinus* + (*Pthirus* + *Pediculus*) (20–25 Ma), and *P. schaeffi* + *P. humanus* (5–7 Ma) (Sukumaran and Holder 2015; Mockford et al. 2013; Johnson et al. 2018b). A maximum root age calibration for the split between Trogiomorpha and the remainder of Psocodea was set to 328 Ma based on a previous dating analysis (Johnson et al. 2018a) and was used to estimate the rate of substitution across the topology. These described calibrations are not completely independent of calibrations previously employed (Johnson et al. 2018a) but do include additional calibration points relevant to our current taxon sampling. A reversible (GTR) model was implemented for the analysis. The stationarity of two separate Markov Chain Monte Carlo (MCMC) runs was visualized with Tracer 1.7.1 (Rambaut et al. 2018).

RESULTS

In total, 2370 genes were successfully aligned yielding a supermatrix of 2,945,181 bp including all three codon positions. Transcriptome and whole genome sequences aligned well, facilitating subsequent phylogenetic analyses. On average, each individual sampled had data present for 95% of genes sampled (Table 1).

Topologies from ML phylogenetic analyses of the concatenated sequence data set varied depending on the methods used for coding or removing nucleotides. Much of this variation centered around the placement of the Amphientometae, an infraorder of Troctomorpha comprising free-living taxa. Amphientometae was recovered as sister to the suborder Psocomorpha with maximum support (100% BS), which contains only nonparasitic taxa, when 1) all nucleotide sites or 2) first and second codon positions were analyzed. However, under degeneracy recoding or analysis of second codon positions only, Amphientometae was recovered as sister to the remainder of the Troctomorpha with maximum support (100% BS), the suborder into which it has traditionally been placed (Fig. 1).

Other than the placement of Amphientometae (i.e., monophyly of Troctomorpha), relationships between the other major lineages within Psocodea were generally stable across analyses. Psocomorpha was always recovered as monophyletic (100% BS). Within Troctomorpha, Phthiraptera (parasitic lice) was always

recovered as monophyletic regardless of coding method (100% BS). The family Liposcelididae was also always recovered as monophyletic and as the sister taxon of all parasitic lice (100% BS) as predicted from morphology (Lyal 1985). Nanopsocetae (Pachytroctidae, Sphaeropsocidae, and Liposcelididae plus Phthiraptera) was also always recovered as monophyletic (100% BS).

Among Phthiraptera, there was variation across analyses in the position of some mammal lice (Anoplura, Trichodectidae, and Rhynchophthirina). In particular, Rhynchophthirina (elephant lice) was sister to the chewing louse family Trichodectidae when all nucleotide sites were analyzed (100% BS). However, under 1) degeneracy coding, 2) first and second codon positions only, and 3) second codon positions only, Rhynchophthirina was recovered as sister to Anoplura (sucking lice) (100% BS). Either of these placements resulted in paraphyly of what is traditionally considered to be Ischnocera (one of the suborders of chewing lice): Trichodectidae (parasitizing mammals) and Philopteridae (parasitizing mainly birds). Thus, our results also support the existence of a larger mammal infesting clade comprising the Trichodectidae, Rhynchophthirina, and Anoplura, which corroborates recent analyses (Allen et al. 2017; de Moya et al. 2019; Song et al. 2019). The other traditional chewing louse suborder, Amblycera, was recovered as monophyletic across all analyses and sister to the remainder of Phthiraptera.

Within the Psocomorpha (bark lice, all free-living), relationships between some infraorders showed variation across analyses. In particular, the infraorder Homilopsocidea was not supported as monophyletic across all ML analyses. Two families of Homilopsocidea (Peripsocidae and Ectopsocidae) were most unstable in their placement and each of them sometimes grouped with the Caeciliusetae depending on the method of analysis. However, despite the poor support for the monophyly of the Homilopsocidea, the infraorder was consistently recovered as sister to other members of the Caeciliusetae across ML analyses (100% BS). The Psocetae and Epipsocetae were recovered as sister taxa across ML analyses (89–100% BS) and together sister to Philotarsetae (100% BS). In general, support values are higher within the Psocomorpha when all nucleotide sites are analyzed with a ML approach. The single sampled member of the Archipsocetae (Archipsocidae)

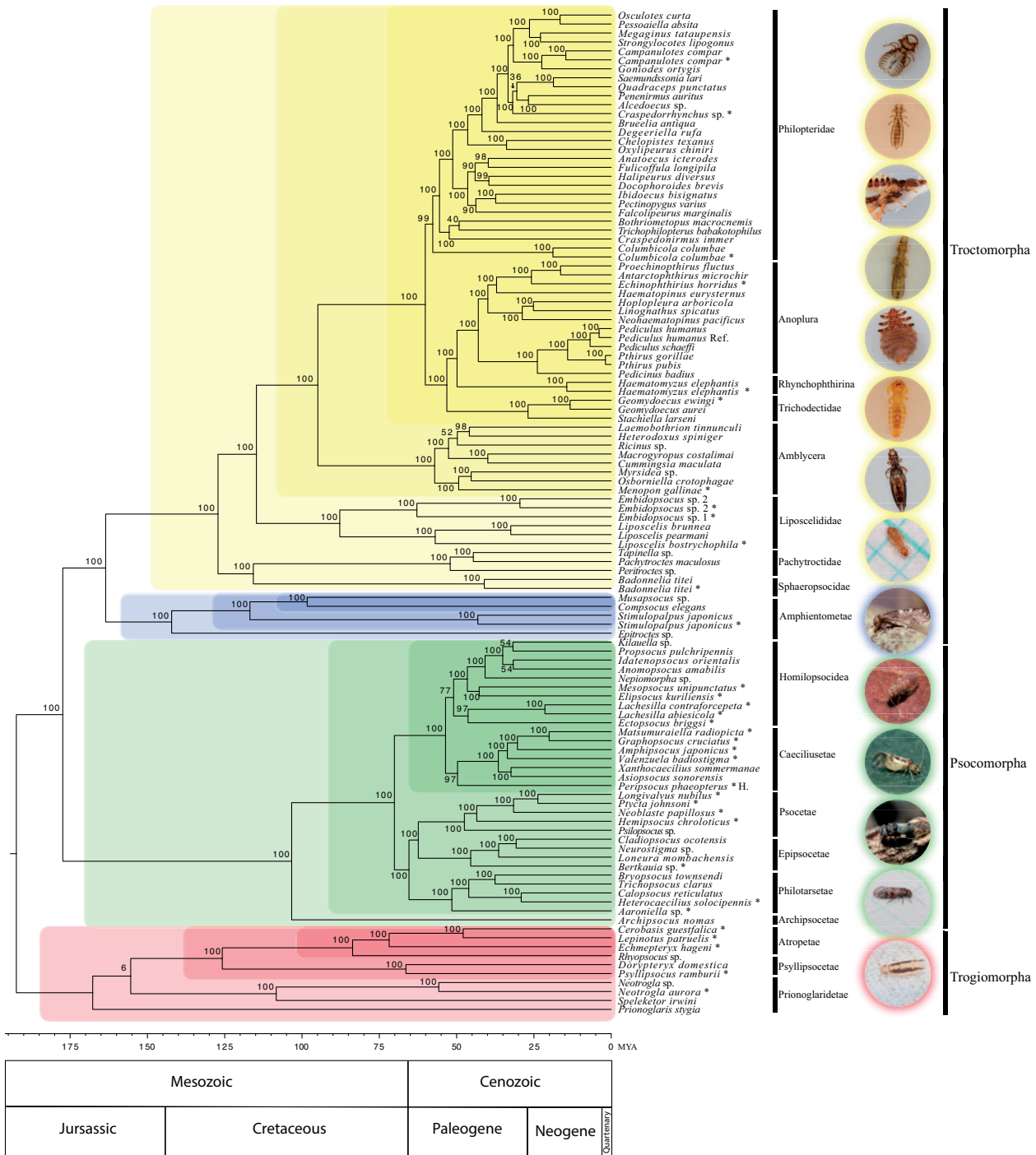


FIGURE 1. The result of phylogenetic analyses using degeneracy recoded nucleotide data. Clade support is depicted as bootstrap support. The timescale provides an estimate of divergences suggested by MCMCtree dating analyses using correlated rates. Taxonomic names marked with an asterisk represent samples that are derived from transcriptomes. Names which lack the asterisk represent samples derived from shotgun whole genome sequencing. The H. following names indicate the taxon is classified within the Homilopsocida.

was always recovered as sister to the remainder of the Psocomorpha (100% BS), as in prior morphological (Yoshizawa 2002) and molecular studies (Yoshizawa and Johnson 2014).

Within the bark louse suborder Trogiomorpha, there was little variation in the results among analyses. The infraorder Prionoglaridetae was recovered as paraphyletic across all analyses, but this paraphyletic relationship

was poorly supported in the degeneracy (6% BS) and second codon position only (33% BS) analyses. However, a paraphyletic Prionoglaridetae was supported with maximum bootstrap support (100% BS) when all nucleotide sites or first and second codon positions were analyzed. The remainder of Trogiomorpha was embedded within this paraphyletic assemblage of Prionoglaridetae. The infraorders Atropetae and Psyllipsocetae were each recovered as monophyletic and sister lineages across all ML analyses (100% BS).

Coalescent gene/species-tree analyses (Astral) of individual gene trees across the 2370 orthologous gene data set yielded similar branching patterns and measures of clade support relative to concatenated ML analyses of the same data type. Most nodes received maximum support (1.0 LPP). As in the ML analyses of all sites for the concatenated data set, coalescent analyses of gene trees from all nucleotide sites display maximum (1.0 LPP) support for a sister relationship between Psocomorpha and Amphientometae (Supplementary Fig. S2 available on Dryad at <https://doi.org/10.5061/dryad.c59zw3r50>). However, when degeneracy recoded gene trees are analyzed (Supplementary Fig. S3 available on Dryad), there is maximum support (1.0 LPP) for a monophyletic Troctomorpha including the Amphientometae. Relationships among members of the Psocomorpha displayed some instability when degeneracy recoded data were analyzed in a coalescent context. However, a similar topology relative to the ML analyses is obtained for members of Psocomorpha when all sites are analyzed in a coalescent context.

Results of four-cluster likelihood-mapping show the distribution of discordant topologies between different methods of analyses for the placement of the Amphientometae (Fig. 2). When all nucleotide sites are analyzed 65.2% of quartets sampled favor a sister relationship between the Amphientometae and Psocomorpha. Similarly, when first and second positions are analyzed the support declines, but 50.2% of quartets still support a sister relationship between the Amphientometae and Psocomorpha. In contrast, when the degeneracy recoded or second codon positions only data are analyzed, 43.8% and 42.5% of quartets sampled respectively, support a sister relationship between the Amphientometae and Nanopsocetae, while only 30.1% and 30.8% support Amphientometae with Psocomorpha.

Quartet sampling analyses are able to assess support from quartets (four-cluster likelihood-mapping) across all nodes in the tree. Using slightly different metrics, these analyses estimate the frequency of discordant topologies across the resultant ML topology tested. When all nucleotide sites are analyzed, a weak majority of quartets support a sister Psocomorpha + Amphientometae (0.23 QC) (Fig. 3). In contrast, when using the degeneracy recoded data set, a slight majority of quartets sampled support a monophyletic Troctomorpha, including the Amphientometae (0.01 QC) (Fig. 4). Quartet sampling also provides an estimate of which nodes are most

stable given the data type and topology analyzed. For example, monophyly of the parasitic louse clade that includes Philopteriidae, Trichodectidae, Anoplura, and Rhynchophthirina is supported by all quartets sampled across all nucleotide sites and degeneracy recoded analyses (1.0 QC) and no discordant topologies are detected (NA QD).

Visualization of the distribution of GC content for first, second, and third codon positions revealed substantial compositional biases at all positions between suborders or infraorders of Psocodea. Third codon positions showed the most variation in compositional biases (Fig. 5). Members of the Amphientometae possess some of the highest levels of GC content for third codon positions, similar to the pattern observed in Psocomorpha. In contrast members of the Nanopsocetae tend to be more AT rich at third codon positions, similar to patterns observed in third codon positions of the Trogiomorpha. First and second codon positions showed similar patterns of compositional biases, but with much lower levels of variance around the medians relative to third positions (Figs. 6 and 7). First codon positions showed more variation in the medians relative to second codon positions. However, members of the Psocomorpha and Amphientometae were suggested to have the highest levels of GC content in first and second positions and the Nanopsocetae and Trogiomorpha tended to be more AT rich in first and second codon positions (Figs. 6 and 7).

Divergence time analysis indicates the main diversification of extant lineages of parasitic lice occurred approximately 60 Ma following the K-PG boundary mass extinction event. The origin of parasitism within Psocodea could have occurred a maximum of 115 Ma (95–148: 95% Myr) based on estimated divergence of the parasitic lineage from nonparasitic members of Psocodea. Divergences between suborders of Psocodea are estimated to have occurred in the lower Jurassic with the deepest split between extant suborders occurring 192 Ma (154–255: 95% Myr) (Fig. 1).

DISCUSSION

Combining Data and Compositional Biases

Few phylogenomic studies have explored the results of combining whole genome and transcriptome-based data (Bossert et al. 2019). Higher-level phylogenomic studies of insects have used transcriptome sequencing to produce large data matrices of thousands of genes (Misof et al. 2014; Peters et al. 2017; Johnson et al. 2018a; Simon et al. 2019; Wipfler et al. 2019). Transcriptome sequencing relies on freshly preserved material, from which RNA can be extracted. Contigs can be annotated for single copy ortholog genes, and methods exist to account for splice variants to resolve these to a single gene sequence (Petersen et al. 2017). New methods have also been developed to individually assemble and annotate single copy genes from shotgun Illumina genome sequences

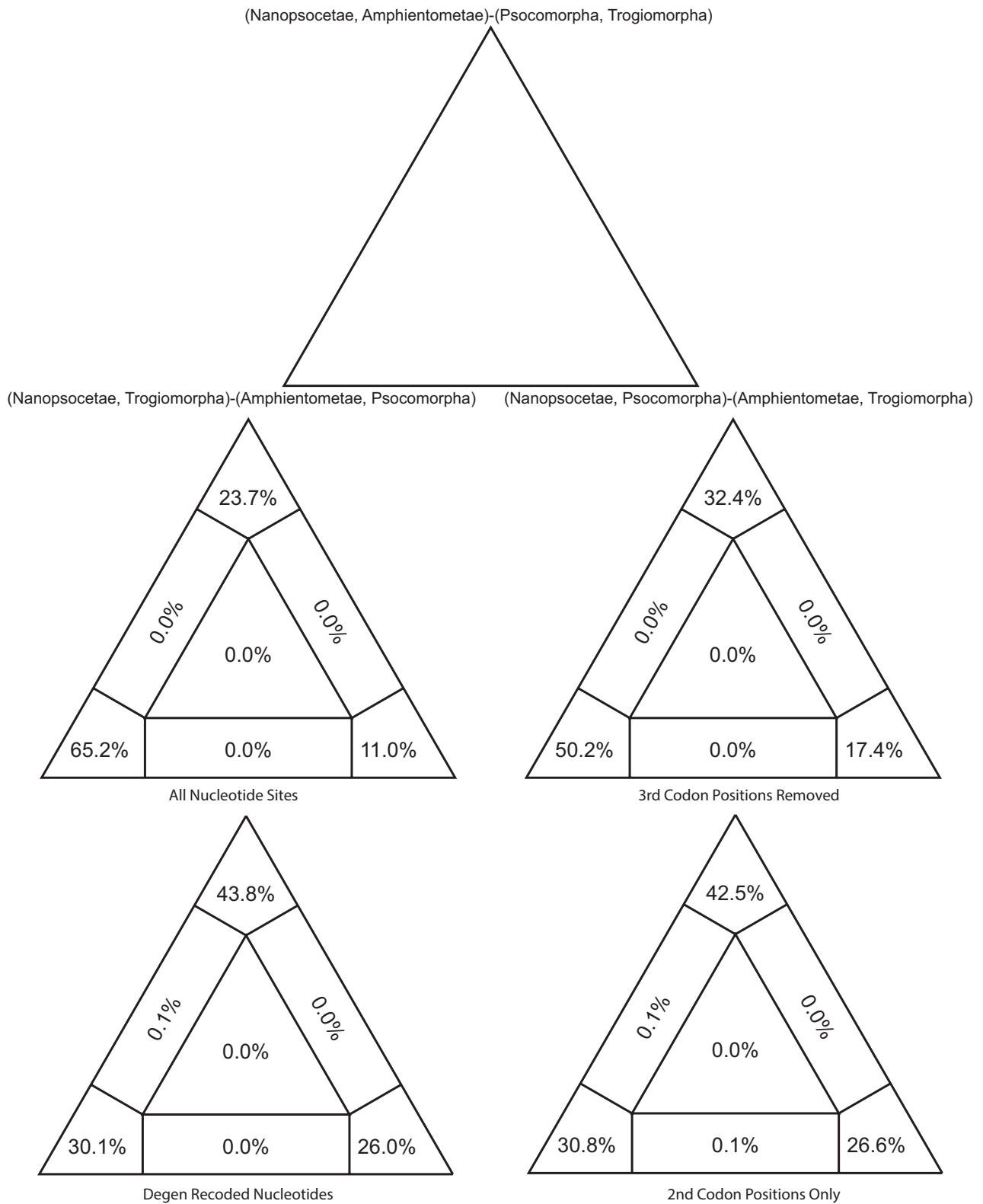


FIGURE 2. The result of likelihood-mapping derived from IQtree. Results show the percentage of quartets derived from analyses supporting relationships among the Trogiomorpha, Psocomorpha, Nanopsocetae, and Amphientometae.

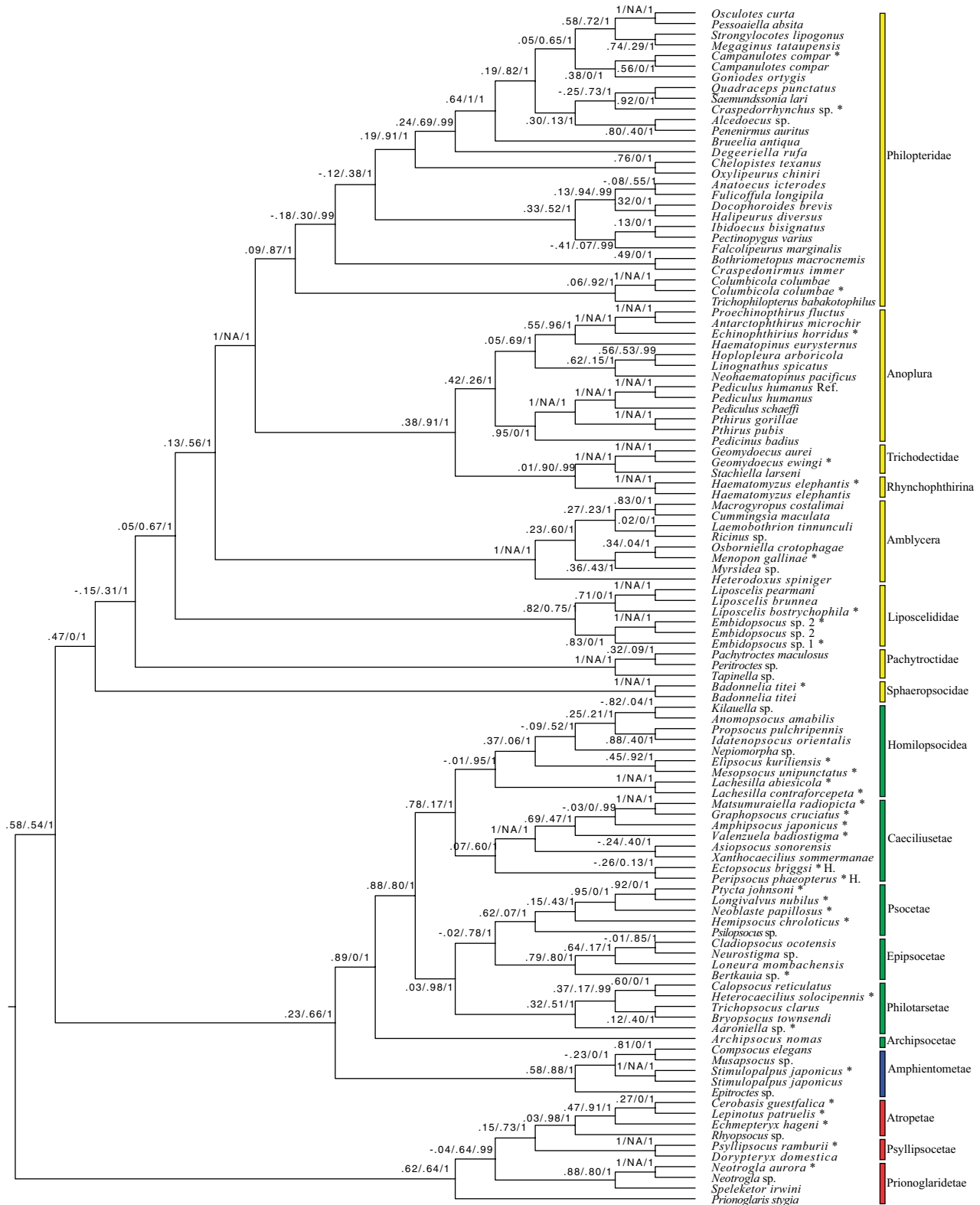


FIGURE 3. A cladogram of the result of quartet sampling based on the analysis of all nucleotide sites. Clade support is depicted as: quartet concordance (QC)/quartet differential (QD)/quartet informativeness (QI). Taxonomic names marked with an asterisk represent samples that are derived from transcriptomes. Names which lack the asterisk represent samples derived from shotgun whole genome sequencing. The H. following names indicate the taxon is classified within the Homilopsocidea.

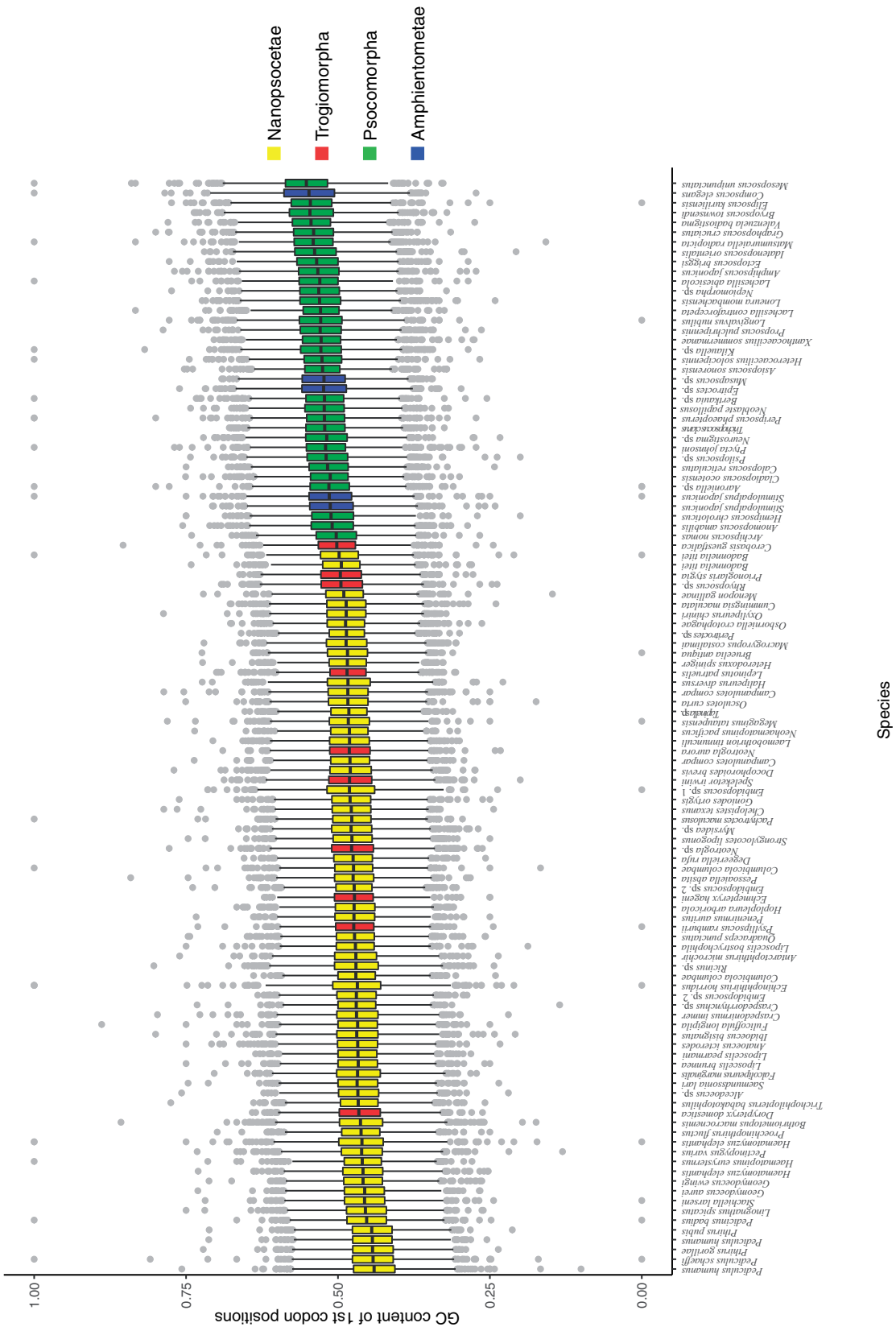


FIGURE 6. Box and whisker plot showing the distribution of GC content in first codon positions from the alignments analyzed.

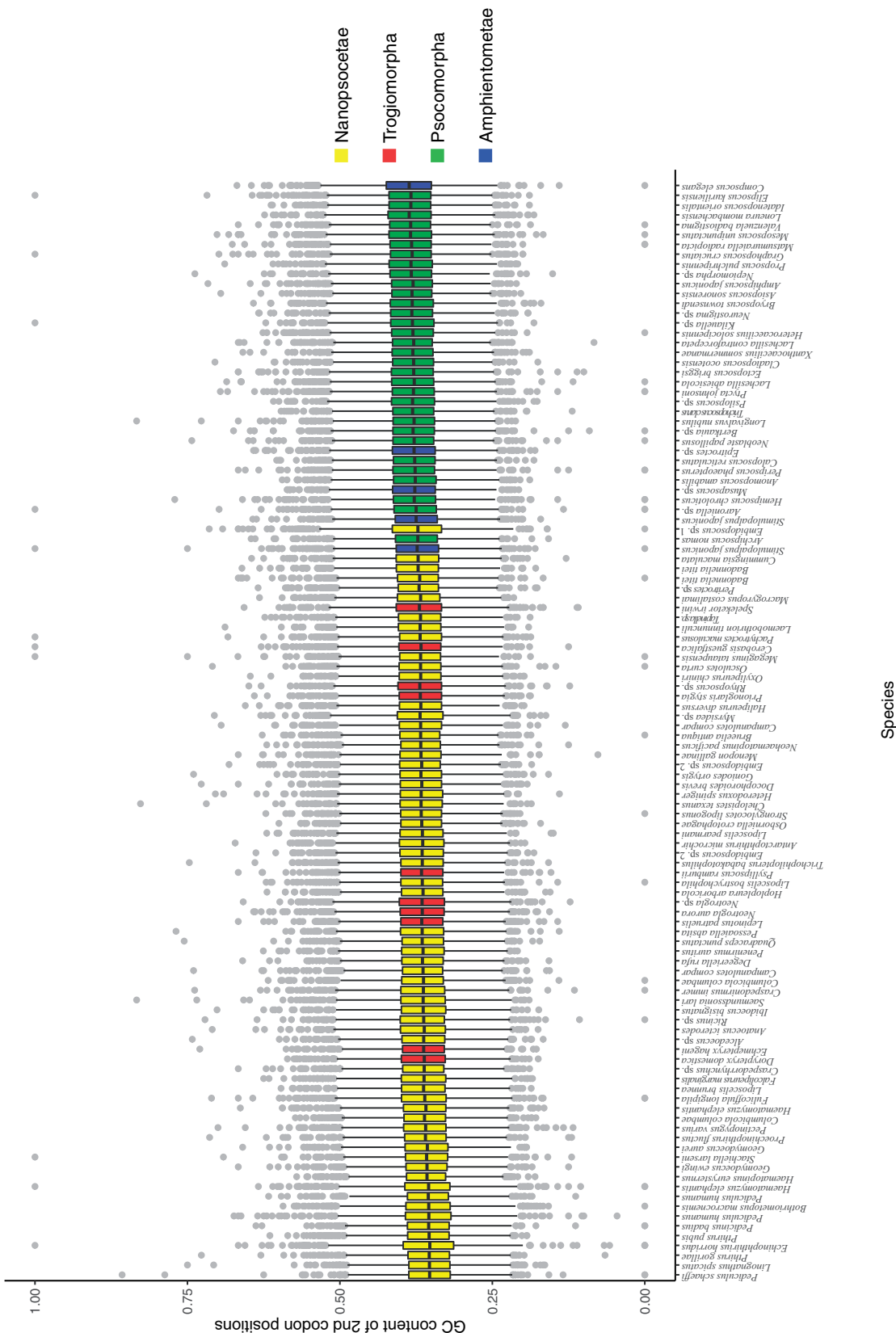


FIGURE 7. Box and whisker plot showing the distribution of GC content in second codon positions from the alignments analyzed.

(Allen et al. 2015, 2017). Whole genome data can include noncoding sequences, but poorly aligned regions can be masked when aligned against transcriptome sequences. Thus, it is possible to combine whole genome and transcriptome data to develop large phylogenomic data sets. Here, we used a customized bioinformatic pipeline to combine transcriptome and genome data to produce a shared set of nuclear orthologs.

Large-scale compositional biases appeared to have some effect on the phylogenetic results for certain taxonomic groups within Psocodea. Most of the instability in our results centered around the placement of Amphientometae, a group of free-living bark lice traditionally placed in the suborder Troctomorpha based upon morphological synapomorphies (Mockford 1993; Lienhard and Smithers 2002; Yoshizawa and Lienhard 2010). However, in our phylogenomic analyses, large base compositional biases resulted in alternative placements of Amphientometae under different nucleotide recoding methods. This is most evident when all nucleotide sites are analyzed in which the Amphientometae are placed with 100% bootstrap support with Psocomorpha, resulting in paraphyly of Troctomorpha. Examination of GC content of third codon positions across the alignment (Fig. 5) shows that Amphientometae are similar in GC composition to Psocomorpha. This same pattern of GC biases is also seen in first and second codon positions (Figs. 6 and 7), although when second codon positions alone are analyzed, Amphientometae is recovered as sister to the remainder of the Troctomorpha, similar to the result using degeneracy recoding. However, when third codon positions are removed, Amphientometae is still placed as the sister of Psocomorpha, suggesting modest base composition biases at first codon positions also affect the results.

Four-cluster likelihood-mapping (quartet mapping) and quartet sampling analyses of the concatenated data demonstrate that quartet-based analyses may also be affected by substantial compositional biases. Likelihood-mapping analyses produce results similar to the ML tree topology itself for a given data type. For example, regarding the position of Amphientometae, degeneracy recoded, and second codon positions produce similar scores and in agreement with the phylogenetic placement of this group with Nanopsocetae (Fig. 2). Degeneracy recodes all nucleotides present in the alignment using IUPAC ambiguity codes so all codons that code for a synonymous mutation are nearly identical (Zwick et al. 2012). This recoding method helps account for the large amount of saturation that can take place at most notably third (Fig. 5) but also first (Fig. 6) codon positions, as well as accounting for some variation in base composition. However, given the similar phylogenetic results when degeneracy recoded and second codon positions only are analyzed, it appears that much of the signal supporting monophyletic Troctomorpha is present in second codon positions. Compositional biases and saturation of third and first codon positions can also skew quartet-based analyses. It appears that the relatively high percent GC

base composition in both Amphientometae and Psocomorpha (blue and green in Figs. 5 and 6), particularly at first and third codon positions, drives the majority of quartets to support a relationship between these two taxa (Fig. 2), similar to the full phylogeny derived from these data types. Although second base positions also show a similar pattern in the ranking of base composition frequencies (blue and green in Fig. 7), this variation spans only a few percent difference and is apparently not enough to influence the resulting tree.

Conflicting topologies in regard to the phylogenetic position of Amphientometae between recoded data types demonstrates the limitations of using a simplified model of evolution when analyzing millions of base pairs of data. Third positions are known to saturate at high rates due to degeneracy of the genetic code that allows for the emergence of silent mutations. This point is obvious when considering that a stable topology is obtained when degeneracy recoded data is analyzed (Fig. 1). Nearly identical results are obtained when second codon positions only are analyzed (Supplementary Fig. S1 available on Dryad). Thus, when phylogenomic analyses are limited by computing power, it may be best to consider alternate methods that reduce data set sizes and recoding strategies to reduce rate heterogeneity and compositional bias that may exist at first and third codon positions between distantly related taxa.

Dating Analysis and the Origin of Parasitism

After accounting for heterogeneity by using the degeneracy recoded matrix, the dating analysis provides insight into the evolution of parasitic and nonparasitic members within Psocodea. We obtained an estimate for some of the earliest divergences within parasitic lice (i.e., shortly after the K-Pg boundary) similar to that found by a recent phylogenomic study (Johnson et al. 2018b) that used mostly calibration points from cospeciation events rather than from fossil free-living bark lice. Our estimate for the earliest divergence within parasitic lice (~100 Ma) was similar to this previous estimate (between 90 and 100 Ma) (Johnson et al. 2018b). The dating estimates completed in this study suggest generally younger origins for nonparasitic members than have been previously reported (Misof et al. 2014; Johnson et al. 2018b; Yoshizawa et al. 2019). The calibrations for analyses produced in this present study are fossil-based minimum age constraints (Mockford et al. 2013) with a maximum age constraint at the root based on previous Bayesian estimates (Johnson et al. 2018a). Differences in calibration methods may account for some of older divergence estimates for nonparasitic members reported in other studies (Misof et al. 2014; Johnson et al. 2018a; Yoshizawa et al. 2019). The dating analysis suggests the origin of parasitism may have occurred a maximum of 115 Ma, predating the K-Pg boundary (66 Ma) (Fig. 1). Our 95% confidence interval for the origin of parasitism also predates the K-Pg boundary (95–148 Ma). Therefore,

TABLE 3. A comparison between historical ordinal taxonomic schemes for Psocoptera and Phthiraptera to the newly proposed classification scheme for a single order Psocodea.

Traditional classification		Newly proposed classification:				
Order	Suborder	Infraorder	Order	Suborder	Infraorder	Parvorder
Psocoptera:			Psocodea:			
	Trogiomorpha:	Prionoglaridetae Psyllipsocetae Atropetae		Trogiomorpha:	Prionoglaridetae Psyllipsocetae Atropetae	
	Psocomorpha:	Archipsocetae Philotarsetae Epipsocetae Psocetae Caeciliusetae Homilopsocidea		Psocomorpha:	Archipsocetae Philotarsetae Epipsocetae Psocetae Caeciliusetae Homilopsocidea	
	Troctomorpha:	Amphientometae Nanopsocetae		Troctomorpha:	Amphientometae Sphaeropsocetae Pachytroctetae Liposcelidetae Phthiraptera:	
Phthiraptera:						Amblycera Anoplura Rhynchophthirina Trichodectera Ischnocera
	Amblycera					
	Anoplura					
	Rhynchophthirina					
	Ischnocera					

it remains a possibility that the ancient host of the first parasitic louse may have been an endothermic dinosaur, although fossil evidence would be needed to confirm this. However, the common ancestor of the clade that eventually evolved parasitism may have been nonparasitic. Therefore, parasitism may have originated anytime between 115 Ma and the initial diversification of parasitic lice (100 Ma).

Implications for the Taxonomic Classification of Psocodea

Our phylogenomic analyses, plus existing morphological evidence (Lyal 1985; Mockford 1993; Yoshizawa and Lienhard 2010) help establish a stable subordinal level classification scheme for the order Psocodea (Table 3). Given that previous analyses have suggested, both based on morphological and molecular evidence, that free-living Psocoptera and parasitic Phthiraptera together form a monophyletic lineage (Lyal 1985; Johnson et al. 2004, 2018a), we recognize Psocodea as a single order encompassing both traditional Psocoptera and Phthiraptera. Below the level of order, the goal of this classification scheme is to reflect the higher-level phylogeny but also retain as many widely used historical names as possible. In particular, given the widespread usage of Phthiraptera, we seek to retain this name, which necessitates changes in taxonomic rank for certain groups within Troctomorpha.

A monophyletic Phthiraptera (parasitic lice) is derived from within the Troctomorpha and sister to the family Liposcelididae across all analyses. All analyses suggest that the origin of parasitism occurred once within the Troctomorpha. Thus, it is necessary to recognize Phthiraptera at a lower taxonomic rank than the suborder Troctomorpha from which these parasites are derived. Given their widespread usage and acceptance (Lienhard and Smithers 2002), we prefer to retain the three historical suborders of bark lice (Trogiomorpha, Psocomorpha, and Troctomorpha) within Psocodea. We prefer to retain the infraordinal taxonomic ranks within Psocomorpha and Trogiomorpha given that these groups are generally supported by our analyses. Given that parasitic lice are also embedded within the traditional Infraorder Nanopsocetae, this would further reduce the rank of Phthiraptera. As a solution to this issue, we elect to divide Nanopsocetae into three infraorders (Table 3). Under this scheme, we also preserve many of the traditional subordinal names within Phthiraptera, and they are now placed at the rank of Parvorder. This scheme also allows us to retain all other existing subordinal parasitic louse names, including Amblycera, Rhynchophthirina, and Anoplura.

One final concern with regards to classification is the status of Ischnocera. Ischnocera (chewing lice) as currently defined (to include both Philopteridae and Trichodectidae) (Price et al. 2003) was paraphyletic across all analyses. This paraphyly has also been detected

in previous studies (Johnson et al. 2018b; Song et al. 2019). Therefore, we suggest that Ischnocera be retained to recognize the bulk of diversity (i.e., Philopteridae, ~3000 species) (Price et al. 2003) and that the Parvorder Trichodectera (Song et al. 2019) be recognized for the less diverse mammal infesting clade Trichodectidae (~400 species) (Price et al. 2003) (Table 3).

SUPPLEMENTARY MATERIAL

Data available from the Dryad Digital Repository: <https://doi.org/10.5061/dryad.c59zw3r50>.

ACKNOWLEDGMENTS

We would like to thank Rodrigo L. Ferreira for field support and supplying samples. We would like to thank Charles Lienhard for information and discussion. We thank the following individuals for assistance in obtaining samples: R. Wilson, D.H. Clayton, T.D. Galloway, E. Osnas, T. Spradling, L. Mugisha, A. K. Saxena, T. Chesser, E. DiBlasi, F. Daunt, V. Smith, R. Furness, E.L. Mockford, J. Jankowski, J.M. Allen, R. Faucett, B. O'Shea, K.G. McCracken, R.E. Junge, J.D. Weckstein, A. Lawrence, K.C. Bell, M.S. Leonardi, and M. Bowser. Photo credit to J. Gausas/Terrestrial Parasite Tracker Project. We thank Thomas Buckley and two anonymous reviewers for comments that helped improve the manuscript.

FUNDING

This work was supported by JSPS (15H04409 and 19H03278 to K.Y.; US NSF DEB-0612938, DEB-1342604, XSEDE DEB-16002, DEB-1855812, and DEB-1925487 to K.P.J.); and US NSF (DEB-1239788 to K.P.J. and C.H.D.).

REFERENCES

- Alkan C., Sajjadian S., Eichler E.E. 2011. Limitations of next-generation genome sequence assembly. *Nat. Methods* 8:61–65.
- Allen J.M., Boyd B., Nguyen N.-P., Vachaspati P., Warnow T., Huang D.I., Grady P.G.S., Bell K.C., Cronk Q.C.B., Mugisha L., Pittendrigh B.R., Leonardi M.S., Reed D.L., Johnson K.P. 2017. Phylogenomics from whole genome sequences using aTRAM. *Syst. Biol.* 66:786–798.
- Allen J.M., Huang D.I., Cronk Q.C., Johnson K.P. 2015. aTRAM - automated target restricted assembly method: a fast method for assembling loci across divergent taxa from next-generation sequencing data. *BMC Bioinformatics* 16.
- Bossert S., Murray E.A., Almeida E.A.B., Brady S.G., Blaimer B.B., Danforth B.N. 2019. Combining transcriptomes and ultraconserved elements to illuminate the phylogeny of Apidae. *Mol. Phylogenet. Evol.* 130:121–131.
- Bossert S., Murray E.A., Blaimer B.B., Danforth B.N. 2017. The impact of GC bias on phylogenetic accuracy using targeted enrichment phylogenomic data. *Mol. Phylogenet. Evol.* 111:149–157.
- Breinholt J.W., Kawahara A.Y. 2013. Phylotranscriptomics: saturated third codon positions radically influence the estimation of trees based on next-gen data. *Genome Biol. Evol.* 5:2082–2092.
- Broadhead E., Richards A.M. 1982. The Psocoptera of East Africa—a taxonomic and ecological survey. *Biol. J. Linn. Soc.* 17:137–216.
- Broadhead E., Wapshere A.J. 1966. Mesopsocus populations on larch in England—the distribution and dynamics of two closely-related coexisting species of Psocoptera sharing the same food resource. *Ecol. Monogr.* 36:327–388.
- Capella-Gutiérrez S., Silla-Martínez J.M., Gabaldón T. 2009. trimAl: a tool for automated alignment trimming in large-scale phylogenetic analyses. *Bioinformatics* 25:1972–1973.
- Clayton D.H., Bush S.E., Johnson K.P. 2015. *Coevolution of life on hosts: integrating ecology and history*. Chicago: University of Chicago Press.
- Cox C.J., Li B., Foster P.G., Embley T.M., Cívado P. 2014. Conflicting phylogenies for early land plants are caused by composition biases among synonymous substitutions. *Syst. Biol.* 63:272–279.
- de Moya R.S. 2020. Psocodea Phylogenomic dataset, v2, Dryad, Dataset, <https://doi.org/10.5061/dryad.c59zw3r50>.
- de Moya R.S., Allen J.M., Sweet A.D., Walden K.K.O., Palma R.L., Smith V.S., Cameron S.L., Valim M.P., Galloway T.D., Weckstein J.D., Johnson K.P. 2019. Extensive host-switching of avian feather lice following the Cretaceous-Paleogene mass extinction event. *Commun. Biol.* 2:1–6.
- Duchêne D.A., Duchêne S., Ho S.Y.W. 2017. New statistical criteria detect phylogenetic bias caused by compositional heterogeneity. *Mol. Biol. Evol.* 34:1529–1534.
- Durden L.A. 2019. Lice (Phthiraptera), Chapter 7. In: Mullen G.R., Durden L.A., editors. *Medical and veterinary entomology*. 8th ed. London, UK: Academic Press. p. 79–106.
- Emeljanov A.F., Golub N.V., Kuznetsova V.G. 2001. Evolutionary transformation of testes and ovaries in booklice, birdlice, and sucking lice (Psocoptera, Phthiraptera: Mallophaga, Anoplura). 81:20.
- Foster P.G., Jermini L.S., Hickey D.A. 1997. Nucleotide composition bias affects amino acid content in proteins coded by animal mitochondria. *J. Mol. Evol.* 44:282–288.
- Galtier N., Gouy M. 1995. Inferring phylogenies from DNA sequences of unequal base compositions. *Proc. Natl. Acad. Sci. USA* 92:11317–11321.
- Gordon A., Hannon G.J. 2010. Fastx-toolkit. http://hannonlab.cshl.edu/fastx_toolkit/index.html
- Houseley J., Tollervey D. 2009. The many pathways of RNA degradation. *Cell* 136:763–776.
- Ishikawa S.A., Inagaki Y., Hashimoto T. 2012. RY-coding and non-homogeneous models can ameliorate the maximum-likelihood inferences from nucleotide sequence data with parallel compositional heterogeneity. *Evol. Bioinformatics Online* 8:EBO.S9017.
- Jarvis E.D., Mirarab S., Aberer A.J., Li B., Houde P., Li C., Ho S.Y.W., Faircloth B.C., Nabholtz B., Howard J.T., Suh A., Weber C.C., Fonseca R.R. da, Li J., Zhang F., Li H., Zhou L., Narula N., Liu L., Ganapathy G., Boussau B., Bayzid M.S., Zavidovych V., Subramanian S., Gabaldón T., Capella-Gutiérrez S., Huerta-Cepas J., Rekepalli B., Munch K., Schierup M., Lindow B., Warren W.C., Ray D., Green R.E., Bruford M.W., Zhan X., Dixon A., Li S., Li N., Huang Y., Derryberry E.P., Bertelsen M.F., Sheldon F.H., Brumfield R.T., Mello C.V., Lovell P.V., Wirthlin M., Schneider M.P.C., Prosdociimi F., Samaniego J.A., Velazquez A.M.V., Alfaro-Núñez A., Campos P.F., Petersen B., Sicheritz-Ponten T., Pas A., Bailey T., Scofield P., Bunce M., Lambert D.M., Zhou Q., Perelman P., Driskell A.C., Shapiro B., Xiong Z., Zeng Y., Liu S., Li Z., Liu B., Wu K., Xiao J., Yinqi X., Zheng Q., Zhang Y., Yang H., Wang J., Smeds L., Rheindt F.E., Braun M., Fjeldsa J., Orlando L., Barker F.K., Jónsson K.A., Johnson W., Koepfli K.-P., O'Brien S., Haussler D., Ryder O.A., Rahbek C., Willerslev E., Graves G.R., Glenn T.C., McCormack J., Burt D., Ellegren H., Alström P., Edwards S.V., Stamatikis A., Mindell D.P., Cracraft J., Braun E.L., Warnow T., Jun W., Gilbert M.T.P., Zhang G. 2014. Whole-genome analyses resolve early branches in the tree of life of modern birds. *Science* 346:1320–1331.
- Jermini L.S., Ho S.Y.W., Ababneh F., Robinson J., Larkum A.W.D. 2004. The biasing effect of compositional heterogeneity on phylogenetic estimates may be underestimated. *Syst. Biol.* 53:638–643.
- Johnson K.P. 2019. Putting the genome in insect phylogenomics. *Curr. Opin. Insect Sci.* 36:111–117.
- Johnson K.P., Cruickshank R.H., Adams R.J., Smith V.S., Page R.D.M., Clayton D.H. 2003. Dramatically elevated rate of mitochondrial

- substitution in lice (Insecta: Phthiraptera). *Mol. Phylogenet. Evol.* 26:231–242.
- Johnson K.P., Dietrich C.H., Friedrich F., Beutel R.G., Wipfler B., Peters R.S., Allen J.M., Petersen M., Donath A., Walden K.K.O., Kozlov A.M., Podsiadlowski L., Mayer C., Meusemann K., Vasilikopoulos A., Waterhouse R.M., Cameron S.L., Weirauch C., Swanson D.R., Percy D.M., Hardy N.B., Terry I., Liu S., Zhou X., Misof B., Robertson H.M., Yoshizawa K. 2018a. Phylogenomics and the evolution of hemipteroid insects. *Proc. Natl. Acad. Sci. USA* 115:12775–12780.
- Johnson K.P., Nguyen N., Sweet A.D., Boyd B.M., Warnow T., Allen J.M. 2018b. Simultaneous radiation of bird and mammal lice following the K-Pg boundary. *Biol. Lett.* 14:20180141.
- Johnson K.P., Yoshizawa K., Smith V.S. 2004. Multiple origins of parasitism in lice. *Proc. R. Soc. B-Biol. Sci.* 271:1771–1776.
- Kearse M., Moir R., Wilson A., Stones-Havas S., Cheung M., Sturrock S., Buxton S., Cooper A., Markowitz S., Duran C., Thierer T., Ashton B., Meintjes P., Drummond A. 2012. Geneious basic: an integrated and extendable desktop software platform for the organization and analysis of sequence data. *Bioinformatics* 28:1647–1649.
- Kozlov A.M., Aberer A.J., Stamatakis A. 2015. ExaML version 3: a tool for phylogenomic analyses on supercomputers. *Bioinformatics* 31:2577–2579.
- Lanfear R., Frandsen P.B., Wright A.M., Senfeld T., Calcott B. 2017. PartitionFinder 2: new methods for selecting partitioned models of evolution for molecular and morphological phylogenetic analyses. *Mol. Biol. Evol.* 34:772–773.
- Laumer C.E., Gruber-Vodicka H., Hadfield M.G., Pearse V.B., Riesgo A., Marioni J.C., Giribet G. 2018. Support for a clade of Placozoa and Cnidaria in genes with minimal compositional bias. *eLife* 7:e36278.
- Lienhard C., Smithers C.N. 2002. Psocoptera (Insecta): world catalogue and bibliography. *Museum d'histoire naturelle, Geneve, Switzerland.*
- Lyal C.H.C. 1985. Phylogeny and classification of the Psocodea, with particular reference to the lice (Psocodea: Phthiraptera). *Syst. Entomol.* 10:145–165.
- Mirarab S., Nguyen N., Guo S., Wang L.-S., Kim J., Warnow T. 2014a. PASTA: ultra-large multiple sequence alignment for nucleotide and amino-acid sequences. *J. Comput. Biol.* 22:377–386.
- Mirarab S., Reaz R., Bayzid M.S., Zimmermann T., Swenson M.S., Warnow T. 2014b. ASTRAL: genome-scale coalescent-based species tree estimation. *Bioinformatics* 30:i541–i548.
- Mirarab S., Warnow T. 2015. ASTRAL-II: coalescent-based species tree estimation with many hundreds of taxa and thousands of genes. *Bioinformatics* 31:i44–i52.
- Misof B., Liu S., Meusemann K., Peters R.S., Donath A., Mayer C., Frandsen P.B., Ware J., Flouri T., Beutel R.G., Niehuis O., Petersen M., Izquierdo-Carrasco F., Wappler T., Rust J., Aberer A.J., Aspöck U., Aspöck H., Bartel D., Blanke A., Berger S., Böhm A., Buckley T.R., Calcott B., Chen J., Friedrich F., Fukui M., Fujita M., Greve C., Grobe P., Gu S., Huang Y., Jermini L.S., Kawahara A.Y., Krogmann L., Kubiak M., Lanfear R., Letsch H., Li Y., Li Z., Li J., Lu H., Machida R., Mashimo Y., Kapli K., McKenna D.D., Meng G., Nakagaki Y., Navarrete-Heredia J.L., Ott M., Ou Y., Pass G., Podsiadlowski L., Pohl H., von Reumont B.M., Schütte K., Sekiya K., Shimizu S., Slipinski A., Stamatakis A., Song W., Su X., Szucsich N.U., Tan M., Tan X., Tang M., Tang J., Timelthaler G., Tomizuka S., Trautwein M., Tong X., Uchifune T., Walz M.G., Wiegmann B.M., Wilbrandt J., Wipfler B., Wong T.K.F., Wu Q., Wu G., Xie Y., Yang S., Yang Q., Yeates D.K., Yoshizawa K., Zhang Q., Zhang R., Zhang W., Zhang Y., Zhao J., Zhou C., Zhou L., Ziesmann T., Zou S., Li Y., Xu X., Zhang Y., Yang H., Wang J., Wang J., Kjer K.M., Zhou X. 2014. Phylogenomics resolves the timing and pattern of insect evolution. *Science* 346:763.
- Mockford E.L. 1993. *North American Psocoptera (Insecta)*. Gainesville, Florida: The Sandhill Crane Press, Inc.
- Mockford E.L., Lienhard C., Yoshizawa K., Mockford E.L., Lienhard C., Yoshizawa K. 2013. Revised classification of “Psocoptera” from Cretaceous amber, a reassessment of published information. *Insecta Matsumurana* 69:1–26.
- New T.R. 1970. The relative abundance of some British Psocoptera on different species of trees. *J. Anim. Ecol.* 39:521–540.
- New T.R. 1987. *Biology of the Psocoptera*. *Orient Insects* 21:1–109.
- Nguyen L.-T., Schmidt H.A., von Haeseler A., Minh B.Q. 2015. IQ-TREE: a fast and effective stochastic algorithm for estimating maximum-likelihood phylogenies. *Mol. Biol. Evol.* 32:268–274.
- Pattengale N.D., Alipour M., Bininda-Emonds O.R.P., Moret B.M.E., Stamatakis A. (2009) How Many Bootstrap Replicates Are Necessary?. In: Batzoglou S. (eds) *Research in Computational Molecular Biology. RECOMB 2009. Lecture Notes in Computer Science*, vol 5541. Springer, Berlin, Heidelberg. https://doi.org/10.1007/978-3-642-02008-7_13
- Pease J.B., Brown J.W., Walker J.F., Hinchliff C.E., Smith S.A. 2018. Quartet sampling distinguishes lack of support from conflicting support in the green plant tree of life. *Am. J. Bot.* 105:385–403.
- Peters R.S., Krogmann L., Mayer C., Donath A., Gunkel S., Meusemann K., Kozlov A., Podsiadlowski L., Petersen M., Lanfear R., Diez P.A., Heraty J., Kjer K.M., Klopstein S., Meier R., Polidori C., Schmitt T., Liu S., Zhou X., Wappler T., Rust J., Misof B., Niehuis O. 2017. Evolutionary history of the Hymenoptera. *Curr. Biol.* 27:1013–1018.
- Petersen, M., Meusemann, K., Donath, A. et al. Orthograph: a versatile tool for mapping coding nucleotide sequences to clusters of orthologous genes. *BMC Bioinformatics* 18, 111 (2017). <https://doi.org/10.1186/s12859-017-1529>.
- Philippe H., Brinkmann H., Lavrov D.V., Littlewood D.T.J., Manuel M., Wörheide G., Baurain D. 2011. Resolving difficult phylogenetic questions: why more sequences are not enough. *PLoS Biol.* 9:e1000602.
- Posada D., Crandall K.A. 1998. MODELTEST: testing the model of DNA substitution. *Bioinformatics* 14:817–818.
- Price R.D., Hellenthal R.A., Palma R.L., Johnson K.P., Clayton D.H. 2003. Chewing lice: world checklist and biological overview. Champaign, IL: Illinois Natural History Survey.
- Prum R.O., Berv J.S., Dornburg A., Field D.J., Townsend J.P., Lemmon E.M., Lemmon A.R. 2015. A comprehensive phylogeny of birds (Aves) using targeted next-generation DNA sequencing. *Nature* 526:569–573.
- Rambaut A., Drummond A.J., Xie D., Baele G., Suchard M.A. 2018. Posterior summarization in Bayesian phylogenetics using tracer 1.7. *Syst. Biol.* 67:901–904.
- Regier J.C., Shultz J.W., Zwick A., Hussey A., Ball B., Wetzer R., Martin J.W., Cunningham C.W. 2010. Arthropod relationships revealed by phylogenomic analysis of nuclear protein-coding sequences. *Nature* 463:1079–1083.
- Romiguier J., Cameron S.A., Woodard S.H., Fischman B.J., Keller L., Praz C.J. 2016. Phylogenomics controlling for base compositional bias reveals a single origin of eusociality in corbiculate bees. *Mol. Biol. Evol.* 33:670–678.
- Roure B., Philippe H. 2011. Site-specific time heterogeneity of the substitution process and its impact on phylogenetic inference. *BMC Evol. Biol.* 11:17.
- RS Team. 2015. RStudio: integrated development for R. RStudio, PBC, Boston, MA URL <http://www.rstudio.com/>.
- Sayyari E., Mirarab S. 2016. Fast coalescent-based computation of local branch support from quartet frequencies. *Mol. Biol. Evol.* 33:1654–1668.
- Scholtz C.H. 2016. The higher classification of southern African insects. *Afr. Entomol.* 24:545–555.
- Sheffield N.C., Song H., Cameron S.L., Whiting M.F. 2009. Non-stationary evolution and compositional heterogeneity in beetle mitochondrial phylogenomics. *Syst. Biol.* 58:381–394.
- Simion P., Philippe H., Baurain D., Jager M., Richter D.J., Di Franco A., Roure B., Satoh N., Quéinnec É., Ereskovsky A., Lapébie P., Corre E., Delsuc F., King N., Wörheide G., Manuel M. 2017. A large and consistent phylogenomic dataset supports sponges as the sister group to all other animals. *Curr. Biol.* 27:958–967.
- Simmons M.P. 2017. Relative benefits of amino-acid, codon, degeneracy, DNA, and purine-pyrimidine character coding for phylogenetic analyses of exons. *J. Syst. Evol.* 55:85–109.
- Simon S., Blanke A., Meusemann K. 2018. Reanalyzing the Palaeoptera problem - the origin of insect flight remains obscure. *Arthropod. Struct. Dev.* 47:328–338.

- Simon S, Letsch H, Bank S, Buckley TR, Donath A, Liu S, Machida R, Meusemann K, Misof B, Podsiadlowski L, Zhou X, Wipfler B and Bradler S (2019) Old World and New World Phasmatodea: Phylogenomics Resolve the Evolutionary History of Stick and Leaf Insects. *Front. Ecol. Evol.* 7:345. doi: 10.3389/fevo.2019.00345
- Simpson J.T., Wong K., Jackman S.D., Schein J.E., Jones S.J.M., Birol Y. 2009. ABySS: a parallel assembler for short read sequence data. *Genome Res.* 19:1117–1123.
- Skinner R.K., Dietrich C.H., Walden K.K.O., Gordon E., Sweet A.D., Podsiadlowski L., Petersen M., Simon C., Takiya D.M., Johnson K.P. 2020. Phylogenomics of Auchenorrhyncha (Insecta: Hemiptera) using transcriptomes: examining controversial relationships via degeneracy coding and interrogation of gene conflict. *Syst. Entomol.* 45:85–113.
- Slater G.S.C., Birney E. 2005. Automated generation of heuristics for biological sequence comparison. *BMC Bioinformatics* 6:31.
- Song F., Li H., Liu G.-H., Wang W., James P., Colwell D.D., Tran A., Gong S., Cai W., Shao R. 2019. Mitochondrial genome fragmentation unites the parasitic lice of Eutherian mammals. *Syst. Biol.* 68:430–440.
- Stamatakis A. 2014. RAxML version 8: a tool for phylogenetic analysis and post-analysis of large phylogenies. *Bioinformatics* 30:1312–1313.
- Strimmer K., Haeseler A. von. 1997. Likelihood-mapping: a simple method to visualize phylogenetic content of a sequence alignment. *Proc. Natl. Acad. Sci. USA* 94:6815–6819.
- Sukumaran J., Holder M.T. 2015. SumTrees: phylogenetic tree summarization. 4.0.0. Available from: <https://github.com/jeetsukumar/DendroPy>.
- Vaidya G., Lohman D.J., Meier R. 2011. SequenceMatrix: concatenation software for the fast assembly of multi-gene datasets with character set and codon information. *Cladistics* 27:171–180.
- Vasilikopoulos A., Balke M., Beutel R.G., Donath A., Podsiadlowski L., Pflug J.M., Waterhouse R.M., Meusemann K., Peters R.S., Escalona H.E., Mayer C., Liu S., Hendrich L., Alarie Y., Bilton D.T., Jia F., Zhou X., Maddison D.R., Niehuis O., Misof B. 2019. Phylogenomics of the superfamily Dytiscoidea (Coleoptera: Adephaga) with an evaluation of phylogenetic conflict and systematic error. *Mol. Phylogenet. Evol.* 135:270–285.
- Wang R., Yao Y., Ren D., Shih C. 2019. Psocoptera – Barklice and Booklice. Rhythms of insect evolution. Chichester, West Sussex, UK:Wiley. p. 185–188.
- Wappler T., Smith V.S., Dalgleish R.C. 2004. Scratching an ancient itch: an Eocene bird louse fossil. *Proc. R. Soc. B Biol. Sci.* 271:S255–S258.
- Wipfler B., Letsch H., Frandsen P.B., Kapli P., Mayer C., Bartel D., Buckley T.R., Donath A., Ederly-Rooks J.S., Fujita M., Liu S., Machida R., Mashimo Y., Misof B., Niehuis O., Peters R.S., Petersen M., Podsiadlowski L., Schütte K., Shimizu S., Uchifune T., Wilbrandt J., Yan E., Zhou X., Simon S. 2019. Evolutionary history of Polyneoptera and its implications for our understanding of early winged insects. *Proc. Natl. Acad. Sci. USA* 116:3024–3029.
- Yang Z. 2007. PAML 4: phylogenetic analysis by maximum likelihood. *Mol Biol Evol.* 24:1586–1591.
- Yoshizawa K. 2002. Phylogeny and higher classification of suborder Psocomorpha (Insecta: Psocodea: 'Psocoptera'). *Zool. J. Linn. Soc.* 136:371–400.
- Yoshizawa K., Johnson K.P. 2010. How stable is the "Polyphyly of Lice" hypothesis (Insecta: Psocodea)? A comparison of phylogenetic signal in multiple genes. *Mol. Phylogenet. Evol.* 55:939–951.
- Yoshizawa K., Johnson K.P. 2013. Changes in base composition bias of nuclear and mitochondrial genes in lice (Insecta: Psocodea). *Genetica* 141:491–499.
- Yoshizawa K., Johnson K.P. 2014. Phylogeny of the suborder Psocomorpha: congruence and incongruence between morphology and molecular data (Insecta: Psocodea: 'Psocoptera'). *Zool. J. Linn. Soc.* 171:716–731.
- Yoshizawa K., Lienhard C. 2010. In search of the sister group of the true lice?: a systematic review of booklice and their relatives, with an updated checklist of Liposcelididae (Insecta: Psocodea). *Arthropod. Syst. Phylogeny* 68:181–195.
- Yoshizawa K., Lienhard C., Johnson K.P. 2006. Molecular systematics of the suborder Trogiomorpha (Insecta: Psocodea: 'Psocoptera'). *Zool. J. Linn. Soc.* 146:287–299.
- Yoshizawa K., Lienhard C., Yao I., Ferreira R.L. 2019. Cave insects with sex-reversed genitalia had their most recent common ancestor in West Gondwana (Psocodea: Prionoglarididae: Speleketorinae). *Entomol. Sci.* 22:334–338.
- Zwick A., Regier J.C., Zwickl D.J. 2012. Resolving discrepancy between nucleotides and amino acids in deep-level arthropod phylogenomics: differentiating serine codons in 21-amino-acid models. *PLoS One* 7:e47450.